ACS APPLIED MATERIALS & INTERFACES

LETTER

www.acsami.org

# Hierarchical Mesoporous Silica Nanotubes Derived from Natural Cellulose Substance

Yanhua Zhang, Xiaoyan Liu, and Jianguo Huang*

Department of Chemistry, Zhejiang University, Hangzhou, Zhejiang 310027, China

Supporting Information

**ABSTRACT:** Bioinspired synthesis of hierarchical mesoporous silica nanotubes by using natural cellulose substance (filter paper) and cetyltrimethylammonium bromide (CTAB) micelles as dual templates was achieved. CTAB micelles were adsorbed onto the surfaces of ultrathin titania film precoated cellulose nanofibers, followed by hydrolysis and condensation of tetraethyl orthosilicate around these micelles to form silica. After calcination and sulfuric acid treatment to remove the organic templates and the thin titania film, bulk white sheets composed of natural hierarchical silica nanotubes with mesopores in the walls were obtained, to which silver nanoparticles were further induced to give a silica-nanotube/metal-nanoparticle hybrid.

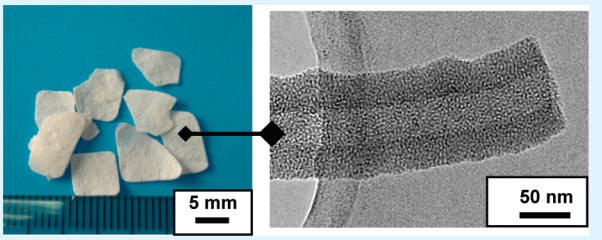


**KEYWORDS:** mesoporous silica, silica nanotube, template synthesis, cellulose, sol−gel

Structurally well-defined silica materials have been recently heatedly pursued, among which mesoporous silica matters,[1−5] and one-dimensional inorganic hollow silica nanotubes[6] are especially interesting. Mesoporous silicas exhibit specific properties including large pore volume, uniform pore-size distribution, large specific surface area, and high surface reactivity,[1−5] which provide wide potentials in industrial and technological applications.[7−11] On the other hand, the silica nanotubes possess unique features like biocompatibility, insulating property, hydrophilic nature, easiness to form colloidal suspension, and facile surface functionalization of their outer and inner walls with desired functional molecules. In the past years, a large variety of silica nanotubes with different morphologies and structures have been synthesized.[6,12−15] Merging of the mesoporous structures and the nanotube morphologies would give rise to a new class of multifunctional silica materials. Triggered by the synthesis of tubular silica with MCM-41 type pores in the wall by Mou's group,[16] a series of mesoporous nanotubular silica materials with excellent properties were reported.[17−20] In these processes, tubular structures were achieved through sol−gel method based template synthesis using surfactants,[16] supermolecular aggregates[17] or carbon nanotubes,[18−20] as templates. However, the simple morphology of those artificial template substrates severely limits the variety of structural types of the products. Biotemplate strategy is a short-cut to yield functional materials with complex natural hierarchical three-dimensional structures that are generally difficult to prepare even with the most technologically advanced synthetic methodologies.[21,22] For example, natural cellulose substances such as filter paper and cotton possess a macro to nanoscopic random morphological hierarchy consisted of $\beta$-D-glucose chain polymers. Replication of this highly sophisticated natural hierarchical network at nanometer level was realized previously by coating ultrathin metal oxide gel films on each cellulose nanofiber surface via the surface sol−gel process.[21] By using this approach, mesoporous silica nanotubes with an astonishing variety of functional nanostructures can be resulted. In the present work, mesoporous silica nanotube with improved structural feature and complicated hierarchical morphology was successfully produced by the sol−gel method accompanied with biotemplate synthesis. The average size of mesopores in the tube walls is *ca.* 2.1 nm, which is comparative with that of conventional MCM-41, and the average thickness of the tube wall is ca. 30−40 nm. Furthermore, silver nanoparticles with uniform particle size were embedded into the mesoporous walls of the resulting silica nanotubes yielding a nanotube/nanoparticle hybrid.

Scheme 1 illustrates the brief fabrication process of the hierarchical mesoporous silica nanotubes. Common commercial ashless quantitative filter paper was used as the template of the hierarchical nanotubular structure. Each cellulose nanofibers of the filter paper were first coated with ultrathin titania gel films (ca. 2.5 nm thick) through the surface sol−gel method[21−23] using titanium *n*-butoxide as precursor (Scheme 1b). The as-prepared titania precoated filter paper was dried and sniped into several squared fractions of ca. 5 mm ×5 mm. Then these filter paper fractions were immersed into the CTAB alkali solution. The cationic CTAB micelles were adsorbed onto the outer surface of titania precoated cellulose nanofibers, which is negatively charged due to the abundant active hydroxyl groups. When the adsorption−desorption equilibrium between the surfactant micelles on the titania-coated cellulose nanofiber surface and the free micelles in bulk solution is established, a layer of CTAB micelles was formed outside the titania precoated nanofiber (Scheme 1c).

**Received:** July 11, 2011
**Accepted:** August 8, 2011
**Published:** August 08, 2011

**Scheme 1. Schematic Illustration of Synthesis Process of Hierarchical Mesoporous Silica Nanotubes Templated by Natural Cellulose Substance: Photograph of (a) Virginal Filter Paper and (g) the Resultant Bulk White Sheet Composed of Mesoporous Silica Nanotubes; (b−f) Sketch Maps of the Samples Obtained in the Corresponding Steps, Respectively.**[a]

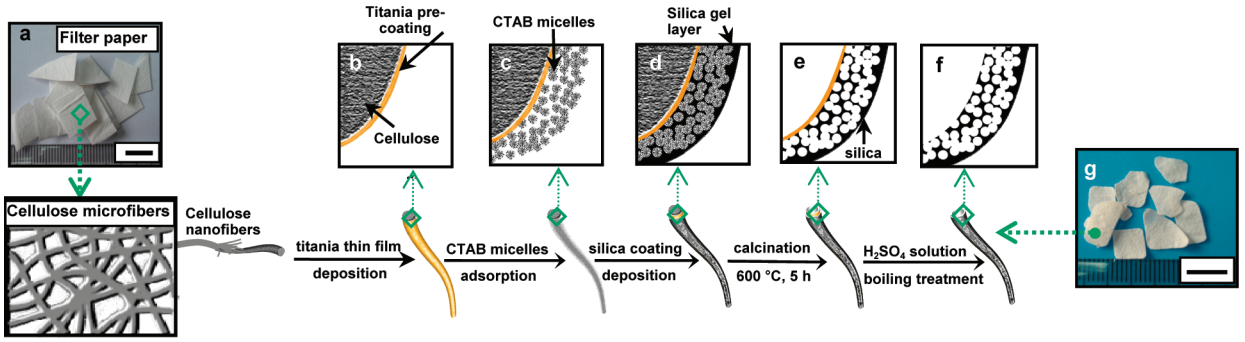


[a] The green arrow represents the enlargement. Scale bars: 1 cm.

Subsequently, tetraethyl orthosilicate (TEOS) was added into the mixture, followed by hydrolysis and condensation. Thus a thin silica film was formed outside the highly concentrated surfactant micelles as well as the titania film precoated cellulose nanofiber surfaces (Scheme 1d). Finally, the as-prepared samples were calcined at 600 °C (heating rate 2 °C/min), resulting in hollow titania/silica composite tubes with large number of mesoporous structures randomly dispersed in the tubular walls (Scheme 1e). The titania film on the inner surface of mesoporous silica nanotube was thoroughly removed by boiling concentrated sulfuric acid treatment for about 20 min, giving bulk white sheets composed of pure mesoporous silica nanotubes (Scheme 1f, g). The resultant hierarchical mesoporous silica nanotubes possess overall morphology of the initial filter paper except for a little shrinkage in size (Scheme 1g; see the Supporting Information for the morphologies of the filter paper employed, Figure S1).

The overview FE-SEM image of the bulk sheet in Scheme 1g shows that the sample consisted of randomly interconnected silica nanotube assemblies with high aspect ratios (Figure 1a). The outer diameters of the nanotubes range from tens to hundreds of nanometers. The highly magnified SEM image of two individual mesoporous silica nanotubes with different diameters clearly exhibits the open ends of the nanotubes (Figure 1b). Figure 1c is the TEM image of an individual mesoporous silica nanotube without concentrated $H_2SO_4$ solution treatment, which indicates that there remains a thin layer of titania (~2.5 nm thickness, as marked in Figure 1c) on the inner side of the silica nanotubes after calcination at 600 °C for 5 h and the sample is mesoporous titania/silica nanotubes composite. This titania layer was completely removed after further boiling concentrated $H_2SO_4$ solution treatment for about 20 min (Figure 1d). XRD analysis (see the Supporting Information, Figure S2) demonstrated the disappearance of the titania precoating layers after the acid treatment and the EDX results (see the Supporting Information, Figure S3) also confirmed that the titania thin film was thoroughly removed. The resulting pure silica nanotube is of uniform wall thickness (30−40 nm) along its entire length (Figure 1d). The inset of Figure 1d indicates that abundant distinct uniform mesopores with average pore size of ca. 2 nm randomly located in the tube walls of the silica nanotubes.

As a control experiment, we tried to fabricate mesoporous silica nanotubes directly using the bare filter paper without titania modification through the identical process. However, no mesoporous nanotubular structure was achieved. It implies that the precoated titania layer plays a critical role in the formation of the expected mesoporous silica nanotubes. The original structure of filter paper is a randomly interconnected network of micro- and nanofibers formed by the sufficient inter- and intramolecular hydrogen bondings, which also contribute to the chemical inertness of cellulose. The titania thin films covering each cellulose nanofiber serve to activate this inert cellulose surface and enhance negative charges, which is favor to deposition of cationic surfactant CTAB micelles on the nanofiber surface. Moreover, the ultrathin nature of the titania film enables the faithful replication of the morphology and structure of the initial filter paper. Only through the titania ultrathin coating, the cationic surfactant CTAB micelles in solution were densely adsorbed onto the negatively charged surface of titania precoated cellulose nanofibers, and silica layer formed coating every cellulose nanofiber as well as adsorbed CTAB micelles after hydrolysis and condensation process.

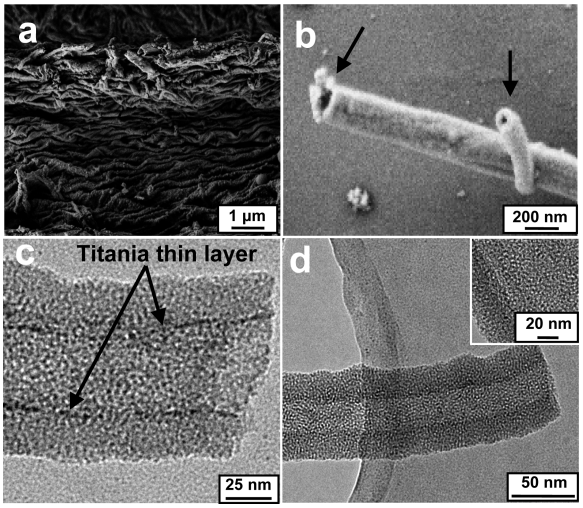


**Figure 1.** (a) Field-emission electron microscopy (FE-SEM) image of the mesoporous silica nanotube sheet, showing nanotube assemblies. (b) FE-SEM image of two individual mesoporous silica nanotubes. (c) Transmission electron microscopy (TEM) image of an isolated mesoporous titania/silica nanotube after calcination, the arrows point out precoated ultrathin titania layer. (d) TEM image of one selected mesoporous silica nanotube resulted after $H_2SO_4$ treatment. The inset in (d) shows the enlarged image of the corresponding sample.

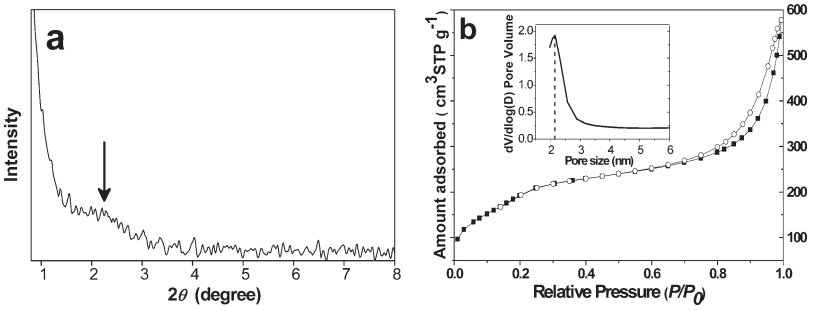


**Figure 2.** (a) Small-angle X-ray diffraction (XRD) pattern and (b) nitrogen adsorption−desorption isotherms of the mesoporous silica nanotubes. The inset of b is the related pore size distribution curve.

As the XRD pattern presented in Figure 2a, the bulk sheet of mesoporous silica nanotubes gives a peak located at about $2\theta$ = 2.1°, which corresponds to but much weaker than the XRD patterns of conventional MCM-41.[1] The materials with such XRD patterns are usually regarded as 'X-ray amorphous' materials which are usually divided into four broad categories like disordered nanocrystalline, glassy, amorphous, and mixed systems.[24,25] The X-ray amorphous pattern appeared here is caused by the short-range order of mesopores in the tube wall. The nitrogen adsorption−desorption isotherm of the mesoporous silica nanotubes (Figure 2b) exhibits a type IV isotherm with two capillary condensation steps in the relative pressure range of 0.2−1.0 ($p/p_0$). The capillary condensation step at relative pressure about 0.3 ($p/p_0$) is a contribution of the typical uniform mesopores in the tube walls. The sharp capillary condensation step occurs in the relative pressure range of 0.7−0.95 ($p/p_0$) due to the existence of macropores in the materials. These results demonstrate the formation of the tubular structure in the corresponding sample. According to the Barrett−Joyner−Halenda (BJH) method, the uniform diameter of the mesopores in the wall of mesoporous silica nanotube is estimated to be about 2.1 nm (sharp peak in the inset of Figure 2b), which is consistent with the TEM observations. The same value is obtained for mesoporous silica particles prepared using CTAB micelles as single template. The BET (Brunauer−Emmett−Teller) surface area of the mesoporous silica nanotube is 765.5 $m^2/g$, which is a little larger than that of mesoporous silica particles synthesized via identical process without employing filter paper (760.5 $m^2/g$). This slight increase in BET surface area is considered because of the unique network structures of the former sample which was inherited from the initial template filter paper, because the surface area of filter paper was reported to be ca. 4 $m^2/g$.[26] Moreover, the sample possesses a much larger pore volume (1.039 $cm^3/g$) than that of mesoporous silica particles (0.349 $cm^3/g$), which indicates that the tubular structure has significant effect on improving the total pore volume of the material.

The mesoporous silica nanotube with large BET surface area provides a practical substrate for immobilization of noble metal particles to be applied as specific catalysts. And immobilization of silver nanoparticles into mesoporous silica matrices has been attracting continuous interests aiming at tailored materials functions.[27−30] Here, Ag nanoparticles were introduced through adsorption and reduction of $AgNO_3$. Figure 3a shows the FE-SEM image of Ag particles incorporated mesoporous silica nanotubes, in which the hierarchical morphology and nanostructure of mesoporous silica nanotubes shown in Figure 1a preserved perfectly. As envisioned in the TEM image (Figure 3b), a large number of

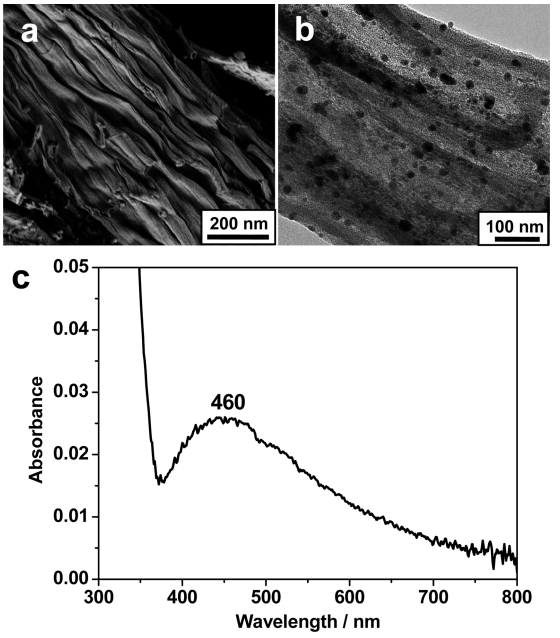


**Figure 3.** (a) FE-SEM micrograph, (b) TEM micrograph, and (c) diffuse reflectance UV−vis spectrum of silver nanoparticles incorporated mesoporous silica nanotubes.

individual Ag nanoparticles with spherical shape are decorated on the surface of each individual mesoporous silica nanotube. The size of these silver nanoparticles on the nanotube surface are relatively uniform, which is measured about 20−30 nm. And the diffuse reflectance UV−vis spectrum of the hybrid shows an absorption band at around 460 nm (Figure 3c), which is the characteristic surface plasmon resonance peak of silver nanoparticles.[31]

In summary, hierarchical mesoporous silica nanotubes were fabricated through a facile and efficient natural template synthesis strategy. While titania precoated common filter paper acts as sophisticated natural structured template for nanotubes, the surfactant CTAB micelles are responsible for forming mesopores in the tube walls. The ultrathin titania precoating, which increased the electronegativity of cellulose nanofibers surface, plays a key role during the adsorption of cationic surfactant micelles on filter paper. The resultant bulk sheet was endowed with not only the tubular structure with tube wall thickness of 30−40 nm but also mesopores of diameter ca. 2.1 nm. This highly porous material shows very large pore volume and specific surface area, which are in favor of introducing functional silver nanoparticles

with regular size. The noble metal nanoparticles uniformly decorated on the tube wall of mesoporous silica nanotube possess great potential applications in catalysis, separation, and delivery fields. The effective approach described here fully take advantage of the two template substrates, and it sheds a considerable light on the design and preparation of highly porous nanotubular materials with hierarchical structures. Moreover, it has been demonstrated that natural cellulose substance such as filter paper serves as attractive templates for the syntheses of various nanostructured metal oxide (hybrid) materials[32−37] as well as polymeric ones.[38−40]

## ■ ASSOCIATED CONTENT

**Supporting Information.** Experimental details, FE-SEM image of bare filter paper, XRD and EDX results of the mesoporous silica nanotubes. This material is available free of charge via the Internet at http://pubs.acs.org/.

## ■ AUTHOR INFORMATION

**Corresponding Author**
*Tel. and Fax: +86-571-8795-1202. E-mail: jghuang@zju.edu.cn.

## ■ ACKNOWLEDGMENT

This work was supported by the National Key Project on Basic Research of China (2009CB930104), Zhejiang Provincial Natural Science Foundation of China (R2080061), and the Chinese Universities Scientific Fund (2010QNA3009).

## ■ REFERENCES

(1) Kresge, C. T.; Leonowicz, M. E.; Roth, W. J.; Vartuli, J. C.; Beck, J. S. *Nature* **1992**, *359*, 710–712.
(2) Tao, C.; Li, J. B. *Langmuir* **2003**, *19*, 10353–10356.
(3) Tüysüz, H.; Lehmann, C. W.; Bongard, H.; Tesche, B.; Schmidt, R.; Schüth, F. *J. Am. Chem. Soc.* **2008**, *130*, 11510–11517.
(4) Yang, Y.; Song, W. X.; Wang, A. H.; Zhu, P. L.; Fei, J. B.; Li, J. B. *Phys. Chem. Chem. Phys.* **2010**, *12*, 4418–4422.
(5) Yang, Y.; Yan, X. H.; Cui, Y.; He, Q.; Li, D. X.; Wang, A. H.; Fei, J. B.; Li, J. B. *J. Mater. Chem.* **2008**, *18*, 5731–5737.
(6) Jung, J. H.; Park, M.; Shinkai, S. *Chem. Soc. Rev.* **2010**, *39*, 4286–4302.
(7) Mal, N. K.; Fujiwara, M.; Tanaka, Y. *Nature* **2003**, *421*, 350–353.
(8) Taylor, K. M. L.; Kim, J. S.; Rieter, W. J.; An, H.; Lin, W. L.; Lin, W. B. *J. Am. Chem. Soc.* **2008**, *130*, 2154–2155.
(9) Scott, B. J.; Wirnsberger, G.; Stucky, G. D. *Chem. Mater.* **2001**, *13*, 3140–3150.
(10) Zhang, Y. H.; Liu, Y. C.; Li, Y. X. *Appl. Catal., A* **2008**, *345*, 73–79.
(11) Corma, A. *Chem. Rev.* **1997**, *97*, 2373–2419.
(12) Zygmunt, J.; Krumeich, F.; Nesper, R. *Adv. Mater.* **2003**, *15*, 1538–1541.
(13) Naito, S.; Ue, M.; Sakai, S.; Miyao, T. *Chem. Commun.* **2005**, 1563–1565.
(14) Fan, R.; Wu, Y. Y.; Li, D. Y.; Yue, M.; Majumdar, A.; Yang, P. D. *J. Am. Chem. Soc.* **2003**, *125*, 5254–5255.
(15) Mitchell, D. T.; Lee, S. B.; Trofin, L.; Li, N. C.; Nevanen, T. K.; Soderlund, H.; Martin, C. R. *J. Am. Chem. Soc.* **2002**, *124*, 11864–11865.
(16) Lin, H. P.; Mou, C. Y. *Science* **1996**, *273*, 765–768.
(17) Yang, S. M.; Sokolov, I.; Coombs, N.; Kresge, C. T.; Ozin, G. A. *Adv. Mater.* **1999**, *11*, 1427–1431.
(18) Ding, K.; Hu, B.; Xie, Y.; An, G.; Tao, R.; Zhang, H.; Liu, Z. *J. Mater. Chem.* **2009**, *19*, 3725–3731.
(19) Yang, Y. K.; Qiu, S. Q.; Cui, W.; Zhao, Q.; Cheng, X. J.; Li, R. K. Y.; Xie, X. L.; Mai, Y. W. *J. Mater. Sci.* **2009**, *44*, 4539–4545.
(20) Bian, S. W.; Ma, Z.; Zhang, L. S.; Niu, F.; Song, W. G. *Chem. Commun.* **2009**, 1261–1263.
(21) Huang, J.; Kunitake, T. *J. Am. Chem. Soc.* **2003**, *125*, 11834–11835.
(22) Huang, J.; Ichinose, I.; Kunitake, T. *Chem. Commun.* **2005**, 1717–1719.
(23) Huang, J.; Ichinose, I.; Kunitake, T.; Nakao, A. *Langmuir* **2002**, *18*, 9048–9053.
(24) Bates, S.; Zografi, G.; Engers, D.; Morris, K.; Crowley, K.; Newman, A. *Pharm. Res.* **2006**, *23*, 2333–2349.
(25) Jacobs, P. A.; Derouane, E. G.; Weitkamp, J. *J. Chem. Soc., Chem. Commun.* **1981**, 591–593.
(26) Kemell, M.; Pore, V.; Ritala, M.; Leskelä, M.; Lindén, M. *J. Am. Chem. Soc.* **2005**, *127*, 14178–14179.
(27) Besson, S.; Gacoin, T; Ricolleaub, C.; Boilot, J.-P. *Chem. Commun.* **2003**, 360–361.
(28) Hornebecq, V.; Antonietti, M.; Cardinal, T.; Treguer-Delapierre, M. *Chem. Mater.* **2003**, *15*, 1993–1999.
(29) Sun, J.; Ma, D.; Zhang, H.; Liu, X.; Han, X.; Bao, X.; Weinberg, G.; Pfänder, N.; Su, D. *J. Am. Chem. Soc.* **2006**, *128*, 15756–15764.
(30) Qi, H.; Shopsowitz, K. E.; Hamad, W. Y.; MacLachlan, M. J. *J. Am. Chem. Soc.* **2011**, *133*, 3728–3731.
(31) Niu, A.; Han, Y. J.; Wu, J. A.; Yu, N.; Xu, Q. *J. Phys. Chem. C* **2010**, *114*, 12728–12735.
(32) Huang, J.; Kunitake, T.; Onoue, S. *Chem. Commun.* **2004**, 1008–1009.
(33) Huang, J.; Matsunaga, N.; Shimanoe, K.; Yamazoe, N.; Kunitake, T. *Chem. Mater.* **2005**, *17*, 3513–3518.
(34) Aoki, Y.; Huang, J.; Kunitake, T. *J. Mater. Chem.* **2006**, *16*, 292–297.
(35) Liu, X.; Gu, Y.; Huang, J. *Chem.—Eur. J.* **2010**, *16*, 7730–7740.
(36) Gu, Y.; Liu, X; Niu, T.; Huang, J. *Chem. Commun.* **2010**, *46*, 6096–6098.
(37) Zhang, Y.; Huang, J. *J. Mater. Chem.* **2011**, *21*, 7161–7165.
(38) Huang, J.; Ichinose, I.; Kunitake, T. *Chem. Commun.* **2005**, 1717–1719.
(39) Gu, Y.; Huang, J. *J. Mater. Chem.* **2009**, *19*, 3764–3770.
(40) Gu, Y.; Niu, T.; Huang, J. *J. Mater. Chem.* **2010**, *20*, 10217–10223.